Suppressing Solid-State Quenching in Red Emitting Conjugated Polymers

Jeroen Royakkers[†‡], Alessandro Minotto[⊥‡], Daniel G. Congrave[†‡], Weixuan Zeng[†], Ali Hassan[⊥], Anastasia Leventis[†], Franco Cacialli[⊥], Hugo Bronstein[†Δ*]

[†]Department of Chemistry, University of Cambridge, Lensfield Road, Cambridge CB2 1EW, United Kingdom.
[Δ]Cavendish Laboratory, University of Cambridge, Cambridge CB3 0HE, United Kingdom.
[⊥]Department of Physics and Astronomy and LCN, University College London, Gower Street, London WC1E 6BT, United Kingdom.

ABSTRACT: Conjugated polymers with intense solid-state emission are vital for the development of next-generation optoelectronic devices. In particular, it remains extremely challenging to construct π-conjugated systems which emit in the red region of the electromagnetic spectrum and also retain their optical properties and intense photoluminescence in the solid state. In this article we report the synthesis and characterization of three novel diketopyrrolopyrrole-based conjugated polymers, with systematic variation of the covalent encapsulation density. Through control of the distance and density of encapsulation, our red-emitting polymers demonstrate that aggregation caused quenching can be mostly eliminated, culminating in the most efficient solid-state photoluminescence from red conjugated polymers to date.

INTRODUCTION

The development of emissive solid-state organic conjugated materials is extremely important due to their versatile use in optoelectronic applications, such as organic light-emitting diodes (OLEDs),[1] luminescent sensors,[2] light-emitting transistors,[3–5] solid-state lasing,[6–8] and biological imaging.[9] Many π-conjugated chromophores exhibit bright photoluminescence (PL) in dilute solution, but diminished PL in the solid state due to aggregation caused quenching (ACQ). As a result, the ratio (Φ_R) between thin film and solution fluorescence quantum yield (i.e. $\Phi_R = \Phi_{F\ Film}/\Phi_{F\ Sol.}$) is typically very low. Addressing this problem through the development of new organic materials which retain their brightness in the solid state is of utmost importance to spearhead next-generation optoelectronic technologies.

Intermolecular communication and ACQ can be suppressed by spatially isolating individual chromophores. Three important strategies employed to supress ACQ in conjugated materials are; (a) non-covalent threading through a macrocycle,[10,11] (b) incorporation of steric bulk[12,13] and (c) covalent encapsulation through alkylene straps[14–17] (Figure 1).

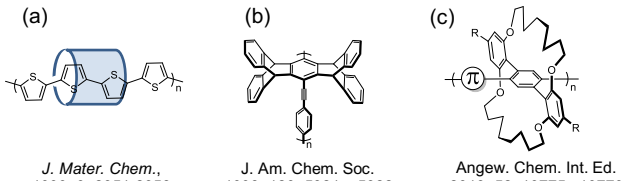

Figure 1. Different strategies employed to prepare shielded conjugated polymers. (a) Non-covalent threading. (b) Incorporation of steric bulk. (c) Covalent encapsulation.

In the past, most encapsulated conjugated materials have been prepared via non-covalent approaches, so as to form rotaxane-like materials.[10,18] Although their synthesis is relatively simple, it is almost impossible to avoid structural defects as their formation is driven thermodynamically.[16] Alternatively, the introduction of bulky side groups can also significantly suppress intermolecular interactions. A recent paper by Würthner and coworkers highlights the potential of this strategy.[13] ACQ was almost completely supressed in a perylene diimide (PDI) dye, which exhibited a solid state Φ_F of over 90%.[13] However, this approach does not always sufficiently limit electronic cross communication,[19] and to the best of our knowledge only very few have been successful in obtaining high values of Φ_R for red emitters through employing steric bulk effects.[20–22]

The third method relies on covalent encapsulation, which has become increasingly popular in the last few years.[14–17,23,24] An interesting study conducted by Kobayashi's group showed that the covalent encapsulation of blue-emitting 9,10-diphenylanthracene gives rise to a very high Φ_F in solution (~98%) and the solid state (~93%), alongside improved photochemical stability.[21] Yet, it remains extremely challenging to achieve similar results for conjugated polymers.

In 2010, Takeuchi's group was one of the first to fully encapsulate a conjugated polymer using the covalent method.[16] Their study made use of alkylene straps to encapsulate two adjacent thiophene units. This in turn locks the thiophene units in place, thereby decreasing rotational motion and lengthening the effective conjugation length (ECL).[16] Later this study was extended to a series of encapsulated phenylene-based polymers.[14] Their only red-emitting polymer had a solution Φ_F of 39%, which quenched to a still impressive solid state Φ_F of 13% (Φ_R = 0.33).[14] This is particularly noteworthy as red-emitting polymers rely on enhanced planarity to achieve a narrow bandgap and hence tend to aggregate more easily at higher concentrations and consequently suffer from quenching.

Based on its potential to overcome ACQ effects in red-emitting polymers, our group sought to extend this promising strategy towards a more relevant building block in optoelectronics. Diketopyrrolopyrrole (DPP) is one of the most popular motifs used in plastic electronics given its versatile industrial use, photochemical stability, bright photoluminescence

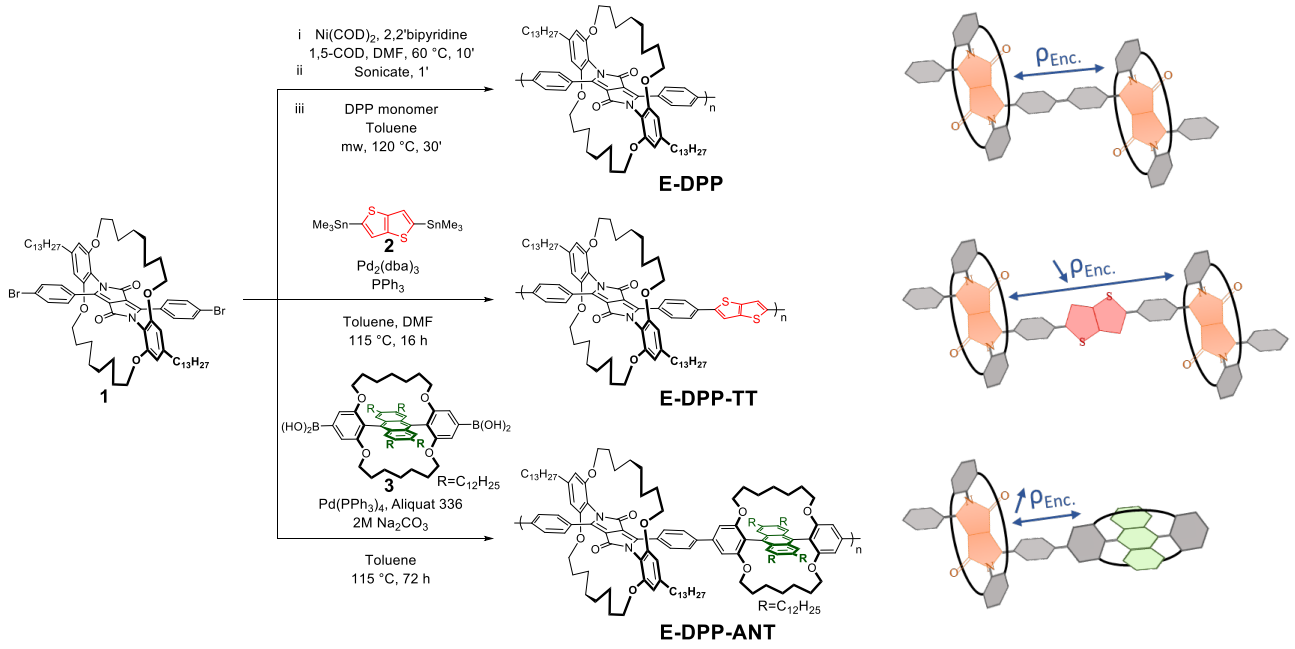

Figure 2. Chemical synthesis of the novel encapsulated DPP polymer series and their corresponding cartoon representation. (Top) **E-DPP** homopolymer. (Middle) **E-DPP-TT** polymer with aromatic spacer. (Bottom) **E-DPP-ANT** polymer with an encapsulated aromatic spacer. ρ_{Enc} stands for density of encapsulation (i.e. more densely encapsulated conjugated polymers are more shielded).

and good electronic properties.[25] Yet, as with most planar building blocks, it suffers from ACQ. Recently, we synthesised a series of encapsulated red-emitting DPP copolymers.[17] The encapsulated polymers displayed more refined spectral features compared to non-encapsulated analogues, indicating the suppression of intermolecular interactions. We observed that encapsulation affords polymers with lower energetic disorder, less conformational defects and enhanced backbone co-linearity. Furthermore, the Φ_F in both solution and solid state increased significantly compared to non-encapsulated analogues.[17] Nevertheless, our reported Φ_R values were consistently below 0.4 and hence it is vital that they are improved.

Herein, we report the synthesis and characterization of three novel encapsulated conjugated polymers with a systematic variation in the extent of encapsulation. We demonstrate that through controlling the density of encapsulation ($\rho_{Enc.}$) it is possible to almost entirely eliminate ACQ in red-emitting conjugated polymers. Furthermore, we report the highest photoluminescence efficiency from a red conjugated polymer in the solid state, to date.

RESULTS & DISCUSSION

Synthesis

The synthesis of the encapsulated phenyl DPP monomer (**1**) (Figure 2) was demonstrated in our previous study.[17] However, the reported preparation is very lengthy, requiring a total of twelve synthetic steps. Instead, we were delighted to discover that a more direct route, where the final three steps (alkylation, Grubbs metathesis and olefin hydrogenation) are replaced by a simple alkylation with 1,8-dibromooctane, afforded the monomer in an almost identical overall yield (3% increase) (Figure S1). Moreover, the requirement for an olefin hydrogenation step is removed, eliminating the risk of problematic monomer dehalogenation side reactions. After the encapsulated DPP monomer was prepared using the improved strategy, it was subjected to homopolymerization under Yamamoto conditions (figure 2) to afford the novel **E-DPP** polymer in excellent yield (92%). **E-DPP** is solely comprised of encapsulated diphenyl DPP units. Hence the encapsulated straps are in very close proximity, separated only by two backbone phenyl rings. Next, we increased the distance between adjacent loops compared to **E-DPP** through incorporation of an aromatic thieno[3,2-b]thiophene spacer (**2**). The **E-DPP-TT** polymer was synthesized using traditional Stille polymerization conditions, again resulting in a near-quantitative yield (97%). Finally, we increased the density of encapsulation compared to **E-DPP** through the use of an orthogonally encapsulated 9,10-diphenylanthracene comonomer (**3**). **E-DPP-ANT** was prepared through Suzuki polycondensation to afford a rubbery polymer in 57% yield after soxhlet extractions. The lower yield for **E-DPP-ANT** is attributed to its higher solubility, which resulted in an increased removal of lower molecular weight polymeric material during the soxhlet purification process. Gel permeation chromatography (GPC) indicated that all polymers were prepared in high number average molecular weights (M_n) well above 20 kDa. The GPC data for the polymers are summarized in table 1.

Table 1. Physical properties of the conjugated DPP polymers.

Polymer	Yield (%)	M_n (kDa)	M_w (kDa)	PDI
E-DPP	92	~80.6	~370.8	4.6
E-DPP-TT	97	~33.4	~113.6	3.4
E-DPP-ANT	57	~55.4	~130.5	2.4

Optical properties

The solution and thin film absorption and emission spectra of the novel DPP polymers are shown in figure 3 and photophysical data are summarized in table 2.

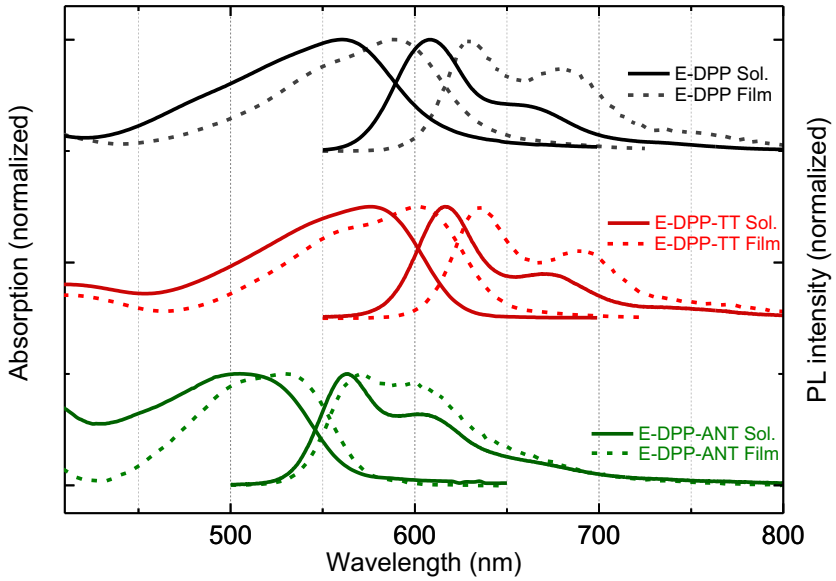

Figure 3. Absorption and photoluminescence profiles of E-DPP (black), E-DPP-TT (red) and E-DPP-ANT (green) in chloroform solution (solid line) and thin film (dashed line).

For **E-DPP**, the solution absorption is relatively featureless with λ_{max} = 560 nm. The PL is sharper and more well resolved with λ_{max} = 609 nm and a secondary peak at ~670 nm corresponding to the 0-1 transition. In thin film, **E-DPP** is a red emitter with a PL λ_{max} of 629 nm and Commission Internationale de l'Éclairage (CIE_{xy}) coordinates of 0.69, 0.31. The solution PL vibronic structure is retained with an enhancement of the 0-1 transition. The absorption profile also displays a slight increase in vibronic fine structure.

The spectral features for **E-DPP-TT** are generally similar to those of **E-DPP**. In solution, the absorption λ_{max} of 576 nm is red-shifted compared to **E-DPP** with a slightly steeper onset, which could be indicative of lower conformational disorder in the ground state.[26,27] The PL is also red-shifted to a λ_{max} of 617 nm and the spectrum looks more resolved compared to **E-DPP**, this time suggesting lower conformational disorder in the excited state.[26,27] These marginal bathochromic shifts are attributed to the more planar nature of the **E-DPP-TT** polymer compared to **E-DPP**. For geometry optimized (B3LYP/6-31G*) trimers (See SI p. S11-12), the dihedral angles are approximately 20º between each diphenyl DPP and TT unit of **E-DPP-TT**, while **E-DPP** is more twisted and displays dihedral angles of approximately 35º between diphenyl DPP units. The experimentally observed red-shifted optical gap of **E-DPP-TT** is also corroborated by the calculated $S_0 \rightarrow S_1$ excitation energies (TD-B3LYP/6-31G*) (Tables S2-4) for the trimers. In thin film, **E-DPP-TT** displays a PL λ_{max} of 636 nm with CIE_{xy} = 0.70, 0.30.

The absorption and PL of **E-DPP-ANT** are substantially blue-shifted compared to both **E-DPP** and **E-DPP-TT** - In thin film **E-DPP-ANT** is an orange emitter with a PL λ_{max} of 570 nm and CIE_{xy} = 0.54, 0.46. This can be rationalized considering the highly twisted nature of this polymer backbone. As well as calculated dihedral angles of ~35º between the DPP and ANT monomers, the encapsulated 9,10-diphenylanthracene has large internal dihedral angles (~80º) between the phenyl and anthracene components (See SI p. S12). This translates to a poorer degree of electronic communication along the polymer backbone and hence widens the optical bandgap. This effect is supported by existing literature as anthracene incorporation has been previously shown to blue-shift DPP polymers.[28,29] Together with the enhanced density of encapsulation and steric shielding (four dodecyl chains per anthracene monomer) encountered in **E-DPP-ANT**, this limited electronic communication is also proposed as an explanation for its minimal solid state red-shift in PL of only 7 nm compared to solution (Figure 3) as the highly twisted conjugated backbone is less likely to planarize or pi-pi stack in the solid state.

In summary, the profiles of the absorption and PL spectra for all polymers provide convincing evidence that the solution optical properties are well retained in the solid state, presumably due to a suppression of interchain interactions through encapsulation. This is particularly apparent from the well-resolved thin film PL spectra which are typically much broader and poorly resolved for non-encapsulated literature polymers, which is associated with aggregation.[30,31]

The solution photoluminescence quantum yields (Φ_F) of the three novel DPP polymers in chloroform, determined using an integrating sphere, are high (> 50%), and remain similarly high in different solvents within experimental error (Table S2). Furthermore, the photoluminescence quantum yields are retained remarkably well in the solid state (up to 41%) for polymers that emit above 560 nm (Table S1).[14,17,32–34] The **E-DPP-TT** copolymer, which features a non-encapsulated aromatic spacer, displays the most intense solution photoluminescence (Φ_F = 71%) of the series. It is quenched to 19% in thin film, corresponding to Φ_R = 0.27. These values are in a similar range to our previously reported analogues that also contain non-encapsulated aromatic spacers.[17]

In comparison, the **E-DPP** homopolymer has a lower solution Φ_F of 51%. However, it displays much lower ACQ in thin film than **E-DPP-TT** having a Φ_F = 32%, which corresponds to

an impressive $\Phi_R = 0.62$. This is attributed to the increased degree of encapsulation in **E-DPP** compared to **E-DPP-TT**. When an encapsulated spacer is included in the **E-DPP-ANT** copolymer, the density of encapsulation increases further. This results in a higher thin film Φ_F of 41% with even lower ACQ ($\Phi_R = 0.72$). Therefore, within this series ACQ is suppressed more effectively as the level of encapsulation increases.

Table 2. Optical properties of orange/red-emitting conjugated DPP-based polymers in this study.

Polymer	State	$\lambda_{abs\ max}$ (nm)	$\lambda_{em\ max}$ (nm)	τ (ns)	τ_{AVG} (ns)	Φ_F (%)	Φ_R
E-DPP	Sol.	560	609	$\tau_1 = 0.54$ (14%) $\tau_2 = 1.76$ (86%)	1.59	51±5[a]	0.62
	Film	589	629	$\tau_1 = 0.04$ (4.2 %) $\tau_1 = 0.53$ (76%) $\tau_2 = 1.39$ (19.8%)	0.68	32±4[a]	
E-DPP-TT	Sol.	576	617	$\tau_1 = 1.19$ (89.3%) $\tau_2 = 3.04$ (10.7%)	1.39	71±7[a]	0.27
	Film	602	636	$\tau_1 = 0.08$ (13%) $\tau_2 = 0.28$ (68.4%) $\tau_3 = 1.57$ (18.6%)	0.49	19±2[a]	
E-DPP-ANT	Sol.	505	563	$\tau_1 = 0.56$ (3.9%) $\tau_2 = 4.60$ (96.1%)	4.44	57±6[a]	0.72
	Film	529	570	$\tau_1 = 0.18$ (5.8%) $\tau_2 = 0.83$ (65.4%) $\tau_3 = 2.11$ (28.8%)	1.16	41±4[a]	

[a]Measured using an integrating sphere. The solutions were measured in dilute chloroform, whereas thin films were spin-coated (800 RPM) from a 10 mg/mL chloroform solution. $\Phi_R = \Phi_{F\ Film}/\Phi_{F\ Sol.}$

Similarly to what is observed for Φ_F, the weighted-average fluorescence lifetimes (τ_{AVG}) (Table 2) decrease when going from solution to thin film for all polymers. A similar observation has been previously reported for other "shielded" conjugated polymers.[35,36] However, we note that τ_{AVG} in thin film decreases to a different extent than is seen in the values of Φ_F. The possibility of interchain in addition to intrachain exciton transfer to either emissive or trap sites, in the solid state, could potentially account for this. However, due to the complex multi-exponential nature of the lifetimes, it is difficult to provide further understanding at this time.

It is important to note that while our results demonstrate that increased encapsulation is highly effective for suppressing ACQ, within our series the more heavily encapsulated **E-DPP** and **E-DPP-ANT** polymers display lower intrinsic (solution) Φ_F (Φ_F = 51 and 57%, respectively) than **E-DPP-TT** (Φ_F = 71%). This indicates that as well as eliminating intermolecular PL quenching pathways, it is possible that encapsulation introduces new intramolecular routes for non-radiative decay. Further investigation is required to determine the exact mechanism. Nevertheless, to the best of our knowledge the thin film Φ_F values reported here are unprecedented for conjugated polymers in this region of the electromagnetic spectrum, as are the high values of Φ_R. Further, we note that this design tactic is superior to non-covalent encapsulation methods as even rotaxane polymers, which are so densely encapsulated they do no quench in solution in the presence of methyl viologen, still aggregate considerably in the solid state ($\Phi_R < 0.5$).[18]

CONCLUSION

We have reported a novel series of encapsulated DPP based conjugated polymers which display the highest solid-state Φ_F ever reported in this region of the electromagnetic spectrum with unprecedentedly suppressed ACQ. The photophysical data support that the encapsulation strategy is highly effective at suppressing intermolecular interactions, enabling the solution photophysical properties of the polymers to be retained in the solid state. This series has enhanced our understanding of how to suppress ACQ in red conjugated polymers by correlating the degree of encapsulation to solid-state Φ_F and Φ_R. Furthermore, we have presented a strategy for efficiently retaining the solution Φ_F of red conjugated polymers in the solid state. In the near future, we aim to further optimize the encapsulating straps to generate π-conjugated systems which have an intrinsic solution Φ_F near unity. Thereby we hope to build upon the advance presented here to develop a platform of super bright solid-state polymeric emitters which bring us closer to emerging next-generation technologies, such as light-emitting transistors or electrically pumped organic lasing.

EXPERIMENTAL SECTION

All reactions were performed in pre-dried glassware under argon atmosphere and with magnetic stirring unless stated otherwise. Light-sensitive reactions were covered in aluminum foil. Chemicals were purchased from chemical suppliers (Merck, TCI, Acros Organics, Alfa Aesar, SLS, Fisher Scientific and Fluorochem) and used as received unless stated otherwise. Reactions were monitored through thin layer chromatography (TLC) using DC Fertigfolien ALUGRAM aluminum sheets coated with silica gel. Column chromatography was carried out using Geduran silica gel 60 (40–63 μm) or Biotage Isolera Four with Biotage SNAP/SNAP ultra cartridges (10, 20, 50, or 100 g). ^{1}H NMR spectra were recorded on a 400 MHz Avance III HD Spectrometer or 400 MHz Smart Probe Spectrometer in the stated solvent using residual protic solvent $CHCl_3$ (δ = 7.26 ppm, s) or DMSO (δ = 2.50 ppm, s) as the internal standard. ^{1}H NMR chemical shifts are reported to the nearest 0.01 ppm and quoted using the following abbreviations: s, singlet; d, doublet; t, triplet; q, quartet; p, pentet; sxt, sextet; m, multiplet. The coupling constants (J) are measured in Hertz. Mass spectra were obtained using a Waters MALDI micro MX spectrometer at the Department of Chemistry, University of Cambridge.

Encapsulated DPP Monomer (1). To a 250 mL round-bottomed flask under argon, DPP tetra-ol (515 mg, 0.5015 mmol), K_2CO_3 (464.4 mg, 3.3601 mmol) and dry DMF (55 mL) were added and the mixture was heated to 50 ºC for 1h. To this, a solution of 1,8-dibromooctane (203 μL, 1.1033 mmol) in dry DMF (55 mL) was added dropwise over 1h. The resulting mixture was heated to 80 ºC and left stirring for 2 days. The reaction mixture was concentrated *in vacuo*, re-dissolved in the minimal amount of chloroform and hexane and purified by column chromatography (using 50 to 70% chloroform in hexane). The product fractions were concentrated in vacuo, sonicated in methanol and dried under high vacuum to yield pure monomer (356.9 mg, 0.2861 mmol, 57%). $\mathbf{R_f}$ = 0.73 (Chloroform); **Mp**: 199-203 °C; **^{1}H NMR** (400 MHz, $CDCl_3$) δ 7.69 (d, J = 8.7 Hz, 4H), 7.39 (d, J = 8.7 Hz, 4H), 6.40 (s, 4H), 3.90 (t, J = 5.1 Hz, 8H), 2.63 – 2.52 (m, 4H), 1.69 – 1.56 (m, 8H), 1.53 – 1.39 (m, 8H), 1.34 – 1.22 (m, 52H), 0.88 (t, J = 6.8 Hz, 6H). **LRMS** (MALDI-TOF): 1248.1 $[M]^+$. Structure supported by **X-ray crystallography**.[1]

Encapsulated Anthracene Monomer (3). The synthesis of this monomer will be reported shortly elsewhere.

E-DPP Polymer. In a nitrogen glovebox, $Ni(COD)_2$ (66.0 mg, 0.24 mmol), and 2,2'-bipyridine (27.7 mg, 0.24 mmol) were added to a 5 mL oven-dried microwave vial and it was sealed. The vial was flushed with argon for 5 minutes and then a solution of 1,5-cyclooctadiene (30 μL, 0.24 mmol) in degassed DMF (970 μL) was added. The resulting mixture was briefly sonicated, stirred at 60 ºC for 10 minutes and briefly sonicated again to obtain a purple coloured mixture. Next, a solution of encapsulated DPP monomer (**1**) (120 mg, 0.0962 mmol) in dry, degassed toluene (5 mL) was added and the reaction mixture was heated in a microwave reactor for 30 minutes at 120 ºC. The resulting red-coloured gelly polymer was dissolved in the minimal amount of chlorobenzene and precipitated into a pre-stirring mixture of methanol (150 mL) and concentrated HCl (10 mL). The resulting solids/flakes were then filtered into a cellulose soxhlet thimble, which was then subjected to soxhlet extractions in acetone (100 ºC), hexane (100 ºC) and chloroform (100 ºC). The chloform fraction was concentrated *in vacuo*, dissolved in the minimal amount of chloroform and precipitated into a pre-stirring mixture of methanol (150 mL) and concentrated HCl (10 mL). After filtration, the polymer was obtained as red/dark pink solids/flakes (96.7 mg, 92% yield); Mn ~80601 Da, Mw ~370820 Da, PDI = 4.601. **Anal. Calcd.** for $C_{72}H_{98}N_2O_6$: C, 79.51; H, 9.08; N, 2.58; O, 8.83. Found: C, 78.89; H, 9.12; N, 2.57 (average of two runs).

E-DPP-TT Polymer. Encapsulated DPP Monomer (**1**) (140 mg, 0.1122 mmol), 2,5-Bis(trimethylstannyl)-thieno[3,2-b]thiophene (52.3 mg, 0.1122 mmol), $Pd_2(dba)_3$ (2.2 mg, 0.0024 mmol) and PPh_3 (2.5 mg, 0.0095 mmol) were placed in a dry 10 mL microwave vial and it was degassed for 45 minutes. Meanwhile, anhydrous toluene and DMF were bubbled with argon (45 min). Next, the degassed anhydrous toluene (2 mL) and DMF (0.2 mL) were added to the monomer/catalyst mixture and it was heated to 115 ºC for 16 h. The gloopy red/pink product was re-dissolved in a minimal amount of chlorobenene and precipitated from stirring methanol (~200 mL) by dropwise addition. The resulting solids were filtered into a soxhlet cellulose thimble and subsequently purified by soxhlet extraction in acetone (100 ºC), hexane (100 ºC) and chloroform (100 ºC). The pink/red chloroform fraction was concentrated *in vacuo*, dissolved in the minimal amount of chlorobenzene, precipiated into stirring methanol and collected by filtration to afford the polymer as a purple flaky solid (134 mg, 97%); Mn ~33365 Da, Mw ~113606 Da, PDI = 3.405. **Anal. Calcd.** for $C_{78}H_{100}N_2O_6S_2$: C, 76.43; H, 8.22; N, 2.29; O, 7.83; S, 5.23. Found: C, 72.73; H, 8.00; N, 2.31 (average of two runs).

E-DPP-ANT. The encapsulated anthracene monomer (**3**) (90.9 mg, 60 µmol), encapsulated DPP monomer (**1**) (75 mg, 60.0 µmol) and $Pd(PPh_3)_4$ (0.7 mg, 0.6 µmol, 1 mol%.) were combined in a 5 mL microwave vial under argon. Degassed toluene (2 mL containing 1 drop of Aliquat 336) and degassed 2 M aqueous Na_2CO_3 (0.27 mL) were then added sequentially to the reaction vial. The resulting mixture was degassed with argon for 10 minutes and then stirred in a preheated 115 °C oil bath for 72 h in the absence of light. The resulting orange-coloured liquid/gel was dissolved in the minimal amount of chlorobenzene and precipitated into a pre-stirring mixture of methanol (150 mL) and concentrated HCl (10 mL). The resulting stringy flakes were then filtered into a cellulose soxhlet thimble, which was then subjected to soxhlet extractions in acetone (100 ºC), hexane (100 ºC) and chloroform (100 ºC). The chloform fraction was concentrated *in vacuo*, dissolved in the minimal amount of chlorobenzene and precipitated into a pre-stirring mixture of methanol (150 mL) and concentrated HCl (10 mL). After filtration, the polymer was obtained as an orange-coloured, rubbery polymer (80.5 mg, 57% yield); Mn ~55355 Da, Mw ~130505 Da, PDI = 2.358. **Anal. Calcd.** for $C_{160}H_{234}N_2O_{10}$: C, 81.93; H, 10.06; N, 1.19; O, 6.82. Found: C, 81.86; H, 9.93; N, 1.18 (average of two runs).

ASSOCIATED CONTENT

Supporting Information. Synthetic Scheme & Characterization, CIE Coordinates, Photophysical and Computational Data.

AUTHOR INFORMATION

Corresponding Author

* E-mail: hab60@cam.ac.uk

Author Contributions

The manuscript was written through contributions of all authors. The others declare no competing financial interest.
‡These authors contributed equally.

ACKNOWLEDGMENT

We gratefully acknowledge funding by EPRSC (Grants EP/P007767/1, EP/S003126/1, and EP/P006280/1) and the Winton Programme for the Physics of Sustainability. FC acknowledges support from the Royal Society for a Royal Society/Wolfson Foundation Research Merit award.

REFERENCES

(1) Gather, M. C.; Köhnen, A.; Meerholz, K. White Organic Light-emitting Diodes. *Adv Mater* **2011**, *23* (2), 233–248.

(2) De Silva, A. P.; Gunaratne, H. Q. N.; Gunnlaugsson, T.; Huxley, A. J. M.; McCoy, C. P.; Rademacher, J. T.; Rice, T. E. Signaling Recognition Events with Fluorescent Sensors and Switches. *Chem Rev* **1997**, *97* (5), 1515–1566.

(3) Capelli, R.; Toffanin, S.; Generali, G.; Usta, H.; Facchetti, A.; Muccini, M. Organic Light-Emitting Transistors with an Efficiency That Outperforms the Equivalent Light-Emitting Diodes. *Nat Mater* **2010**, *9* (6), 496.

(4) Zaumseil, J.; Friend, R. H.; Sirringhaus, H. Spatial Control of the Recombination Zone in an Ambipolar Light-Emitting Organic Transistor. *Nat Mater* **2006**, *5* (1), 69.

(5) Zaumseil, J.; Donley, C. L.; Kim, J.; Friend, R. H.; Sirringhaus, H. Efficient Top-gate, Ambipolar, Light-emitting Field-effect Transistors Based on a Green-light-emitting Polyfluorene. *Adv Mater* **2006**, *18* (20), 2708–2712.

(6) Wang, X.; Liao, Q.; Kong, Q.; Zhang, Y.; Xu, Z.; Lu, X.; Fu, H. Whispering-Gallery-Mode Microlaser Based on Self-Assembled Organic Single-Crystalline Hexagonal Microdisks. *Angew Chemie Int Ed* **2014**, *53* (23), 5863–5867.

(7) Gierschner, J.; Varghese, S.; Park, S. Y. Organic Single Crystal Lasers: A Materials View. *Adv Opt Mater* **2016**, *4* (3), 348–364.

(8) Ramirez, M. G.; Pla, S.; Boj, P. G.; Villalvilla, J. M.; Quintana, J. A.; Díaz-García, M. A.; Fernández-Lázaro, F.; Sastre-Santos, Á. 1, 7-Bay-Substituted Perylenediimide Derivative with Outstanding Laser Performance. *Adv Opt Mater* **2013**, *1* (12), 933–938.

(9) Drummen, G. Fluorescent Probes and Fluorescence (Microscopy) Techniques—illuminating Biological and Biomedical Research. Multidisciplinary Digital Publishing Institute 2012.

(10) Frampton, M. J.; Anderson, H. L. Insulated Molecular Wires. *Angew Chemie Int Ed* **2007**, *46* (7), 1028–1064.

(11) Ching, K. C. Host–guest Complexation: A Convenient Route to Polybithiophene Composites by Electrosynthesis in Aqueous Media. Synthesis and Characterization of a New Material Containing Cyclodextrins. *J Mater Chem* **1999**, *9* (10), 2351–2358.

(12) Yang, J.-S.; Swager, T. M. Porous Shape Persistent Fluorescent Polymer Films: An Approach to TNT Sensory Materials. *J Am Chem Soc* **1998**, *120* (21), 5321–5322.

(13) Schmidt, D.; Stolte, M.; Süß, J.; Liess, A.; Stepanenko, V.; Würthner, F. Protein-like Enwrapped Perylene Bisimide Chromophore as a Bright Microcrystalline Emitter Material. *Angew Chemie Int Ed* **2019**, *58*, 13385 –13389.

(14) Pan, C.; Sugiyasu, K.; Wakayama, Y.; Sato, A.; Takeuchi, M. Thermoplastic Fluorescent Conjugated Polymers: Benefits of Preventing π-π Stacking. *Angew Chemie - Int Ed* **2013**, *52* (41), 10775–10779.

(15) Pan, C.; Zhao, C.; Takeuchi, M.; Sugiyasu, K. Conjugated Oligomers and Polymers Sheathed with Designer Side Chains. *Chem - An Asian J* **2015**, *10* (9), 1820–1835.

(16) Sugiyasu, K.; Honsho, Y.; Harrison, R. M.; Sato, A.; Yasuda, T.; Seki, S.; Takeuchi, M. A Self-Threading Polythiophene: Defect-Free Insulated Molecular Wires Endowed with Long Effective Conjugation Length. *J Am Chem Soc* **2010**, *132* (42), 14754–14756.

(17) Leventis, A.; Royakkers, J.; Rapidis, A. G.; Goodeal, N.; Corpinot, M. K.; Frost, J. M.; Bučar, D.-K. K.; Blunt, M. O.; Cacialli, F.; Bronstein, H. Highly Luminescent Encapsulated Narrow Bandgap Polymers Based on Diketopyrrolopyrrole. *J Am Chem Soc* **2018**, *140* (5), 1622–1626.

(18) Brovelli, S.; Latini, G.; Frampton, M. J.; McDonnell, S. O.; Oddy, F. E.; Fenwick, O.; Anderson, H. L.; Cacialli, F. Tuning Intrachain versus Interchain Photophysics via Control of the Threading Ratio of Conjugated Polyrotaxanes. *Nano Lett* **2008**, *8* (12), 4546–4551.

(19) Zhang, B.; Soleimaninejad, H.; Jones, D. J.; White, J. M.; Ghiggino, K. P.; Smith, T. A.; Wong, W. W. H. Highly Fluorescent Molecularly Insulated Perylene Diimides: Effect of Concentration on Photophysical Properties. *Chem Mater* **2017**, *29* (19), 8395–8403.

(20) Lee, W. W. H.; Zhao, Z.; Cai, Y.; Xu, Z.; Yu, Y.; Xiong, Y.; Kwok, R. T. K.; Chen, Y.; Leung, N. L. C.; Ma, D. Facile Access to Deep Red/near-Infrared Emissive AIEgens for Efficient Non-Doped OLEDs. *Chem Sci* **2018**, *9* (28), 6118–6125.

(21) Qin, W.; Li, K.; Feng, G.; Li, M.; Yang, Z.; Liu, B.; Tang, B. Z. Bright and Photostable Organic Fluorescent Dots with Aggregation-Induced Emission Characteristics for Noninvasive Long-Term Cell Imaging. *Adv Funct Mater* **2014**, *24* (5), 635–643.

(22) Liu, T.; Zhu, L.; Zhong, C.; Xie, G.; Gong, S.; Fang, J.; Ma, D.; Yang, C. Naphthothiadiazole-Based Near-Infrared Emitter with a Photoluminescence Quantum Yield of 60% in Neat Film and External Quantum Efficiencies of up to 3.9% in Nondoped OLEDs. *Adv Funct Mater* **2017**, *27* (12), 1606384.

(23) Royakkers, J.; Minotto, A.; Congrave, D. G.; Zeng, W.; Patel, A.; Bond, A. D.; Bučar, D.-K.; Cacialli, F.; Bronstein, H. Doubly Encapsulated Perylene Diimides: Effect of Molecular Encapsulation on Photophysical Properties. *J Org Chem* **2019**.

(24) Fujiwara, Y.; Ozawa, R.; Onuma, D.; Suzuki, K.; Yoza, K.; Kobayashi, K. Double Alkylene-Strapped Diphenylanthracene as a Photostable and Intense Solid-State Blue-Emitting Material. *J Org Chem* **2013**, *78* (6), 2206–2212.

(25) Liu, Q.; Bottle, S. E.; Sonar, P. Developments of Diketopyrrolopyrrole-Dye-Based Organic Semiconductors for a Wide Range of Applications in Electronics. *Adv Mater* **2020**, *32* (4), 1903882.

(26) Barford, W.; Marcus, M. Perspective: Optical Spectroscopy in π-Conjugated Polymers and How It Can Be Used to Determine Multiscale Polymer Structures. *J Chem Phys* **2017**, *146* (13), 130902.

(27) Panzer, F.; Bässler, H.; Köhler, A. Temperature Induced Order–disorder Transition in Solutions of Conjugated Polymers Probed by Optical Spectroscopy. *J Phys Chem Lett* **2016**, *8* (1), 114–125.

(28) Tieke, B.; Rabindranath, A. R.; Zhang, K.; Zhu, Y. Conjugated Polymers Containing Diketopyrrolopyrrole Units in the Main Chain. *Beilstein J Org Chem* **2010**, *6* (1), 830–845.

(29) Zhu, Y.; Rabindranath, A. R.; Beyerlein, T.; Tieke, B. Highly Luminescent 1, 4-Diketo-3, 6-Diphenylpyrrolo [3, 4-c] Pyrrole-(DPP-) Based Conjugated Polymers Prepared upon Suzuki Coupling. *Macromolecules* **2007**, *40* (19), 6981–6989.

(30) Grell, M.; Bradley, D. D. C.; Ungar, G.; Hill, J.; Whitehead, K. S. Interplay of Physical Structure and Photophysics for a Liquid Crystalline Polyfluorene. *Macromolecules* **1999**, *32* (18), 5810–5817.

(31) Deng, Y.; Yuan, W.; Jia, Z.; Liu, G. H-and J-Aggregation of Fluorene-Based Chromophores. *J Phys Chem B* **2014**, *118* (49), 14536–14545.

(32) Bera, M. K.; Chakraborty, C.; Malik, S. Solid State Emissive Organic Fluorophores with Remarkable Broad Color Tunability Based on Aryl-Substituted Buta-1, 3-Diene as the Central Core. *J Mater Chem C* **2017**, *5* (27), 6872–6879.

(33) Ibnaouf, K. H. Excimer State of a Conjugated Polymer (MEH-PPV) in Thin Films. *Opt Laser Technol* **2013**, *48*, 401–404.

(34) Vithanage, D. A.; Kanibolotsky, A. L.; Rajbhandari, S.; Manousiadis, P. P.; Sajjad, M. T.; Chun, H.; Faulkner, G. E.; O'Brien, D. C.; Skabara, P. J.; Samuel, I. D. W. Polymer Colour Converter with Very High Modulation Bandwidth for Visible Light Communications. *J Mater Chem C* **2017**, *5* (35), 8916–8920.

(35) Yang, J.-S.; Swager, T. M. Fluorescent Porous Polymer Films as TNT Chemosensors: Electronic and Structural Effects. *J Am Chem Soc* **1998**, *120* (46), 11864–11873.

(36) Erdem, T.; Idris, M.; Demir, H. V.; Tuncel, D. Highly Luminescent CB [7]-Based Conjugated Polyrotaxanes Embedded into Crystalline Matrices. *Macromol Mater Eng* **2017**, *302* (11), 1700290.

Insert Table of Contents artwork here

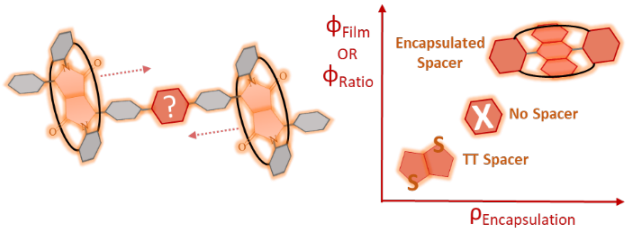

Supplementary Information:

Suppressing Solid-State Quenching in Red Emitting Conjugated Polymers

Jeroen Royakkers[†‡], Alessandro Minotto[⊥‡], Daniel G. Congrave[†‡], Weixuan Zeng[†], Ali Hassan[⊥], Anastasia Leventis[†], Franco Cacialli[⊥], Hugo Bronstein[†Δ*]

[†]Department of Chemistry, University of Cambridge, Lensfield Road, Cambridge CB2 1EW, UK
[Δ]Cavendish Laboratory, University of Cambridge, Cambridge CB3 0HE, UK
[⊥]Department of Physics and Astronomy and LCN, University College London, Gower Street, London WC1E 6BT, UK

Table of Contents

Synthetic Scheme and Characterization

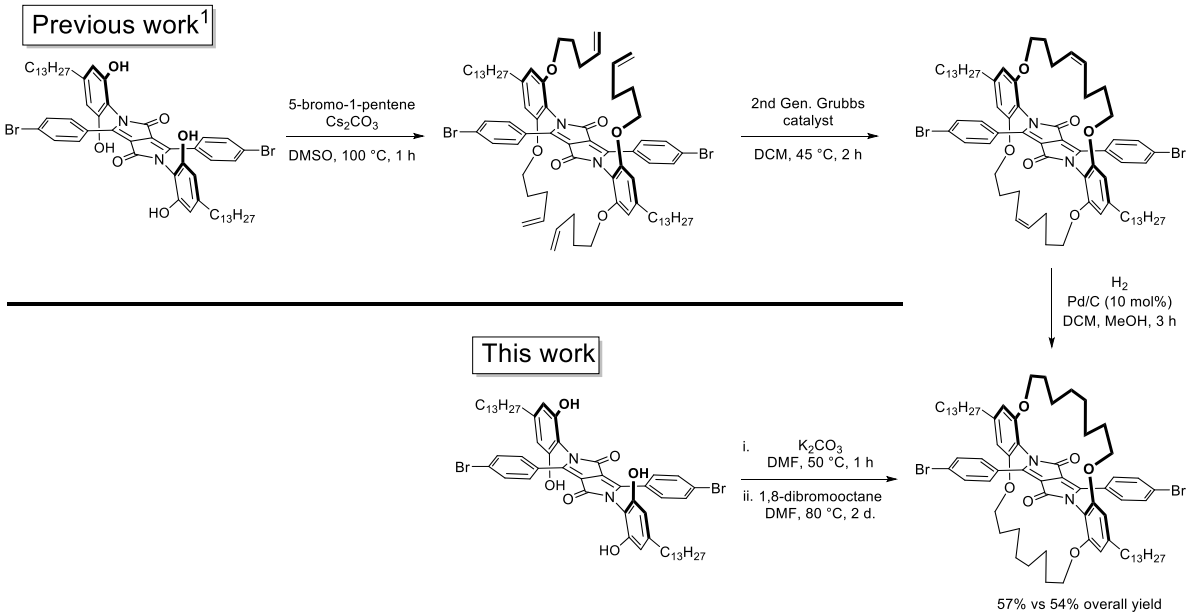

Figure S1. Previous (top)[1] and improved (bottom) synthetic route towards the Encapsulated DPP monomer.

Encapsulated DPP Monomer

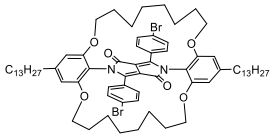

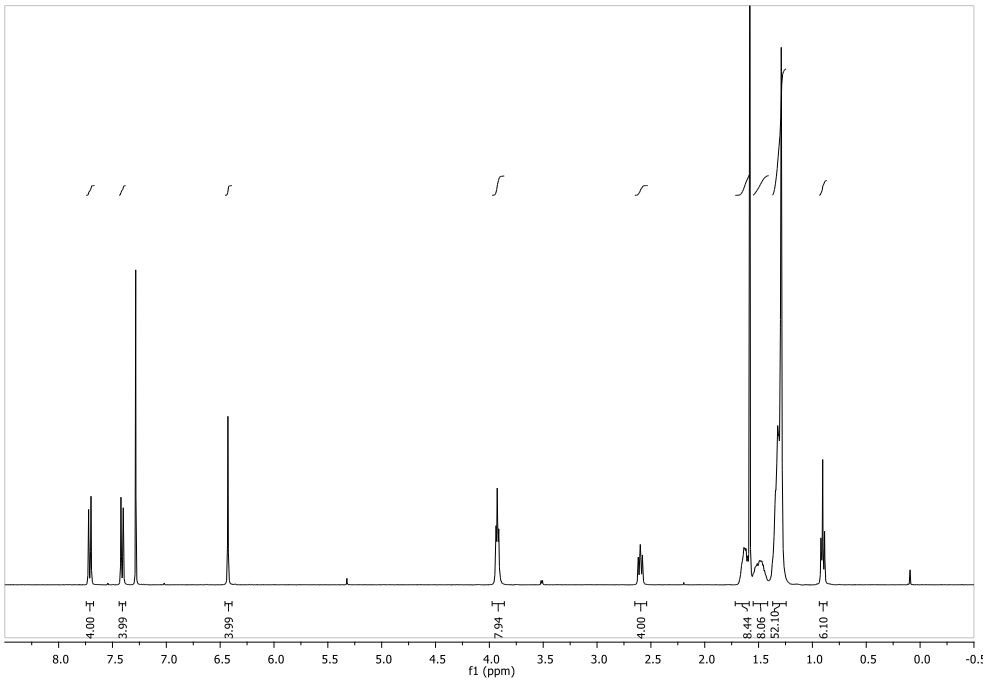

Figure S2. ^{1}H NMR spectrum of the encapsulated DPP monomer.

Summary of Conjugated Polymers Emitting Above 550 nm

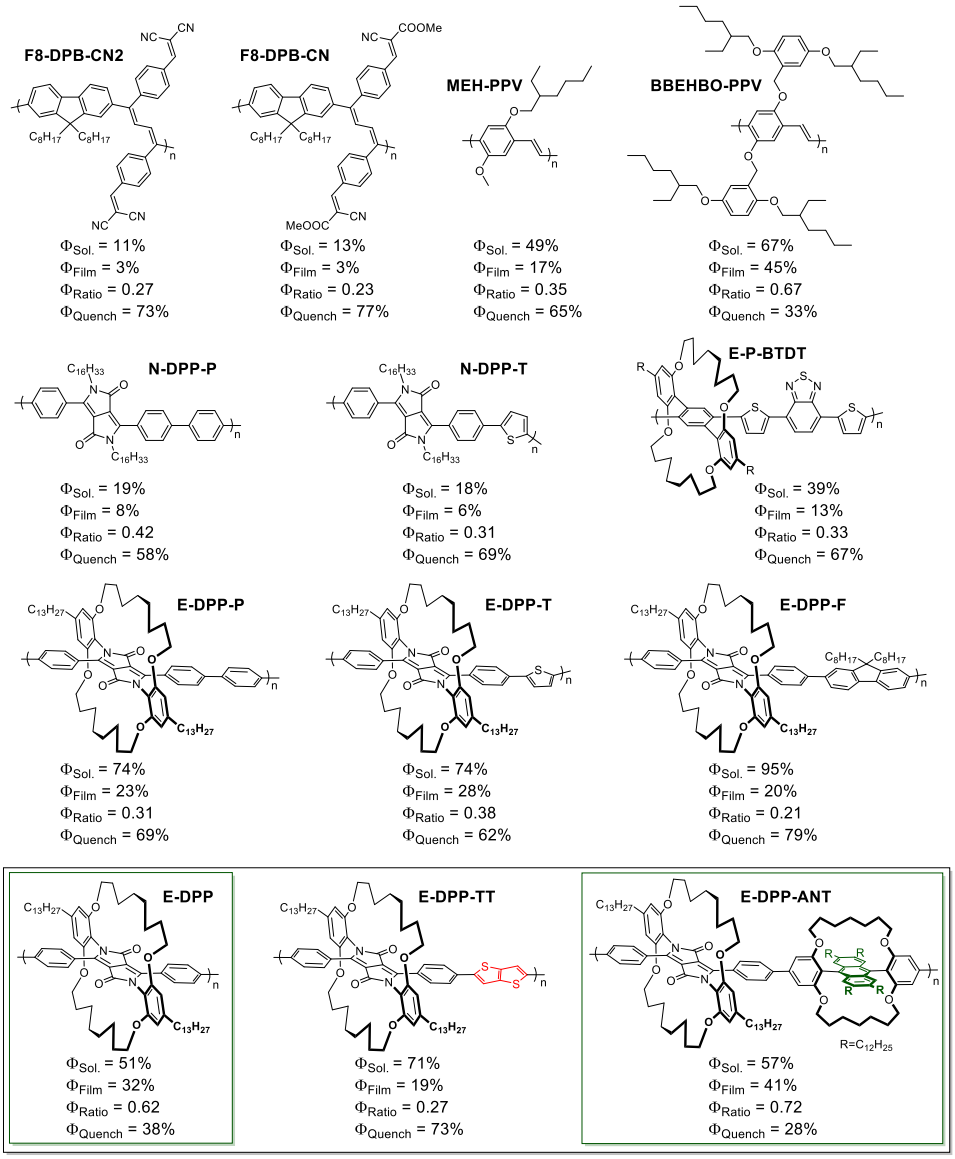

Figure S3. Summary of the PLQY and ACQ data of conjugated polymers including both literature and novel molecules presented in this study.

Table S1. Summary of the optical properties of conjugated polymers which emit above 550 nm from previous literature.

Polymer	State	$\lambda_{em\ max}$ (nm)	Φ_F (%)	Φ_{Ratio}	Φ_{Quench} (%)
E-P-BTDT[2]	Sol.	669	39	0.33	67
	Film	631	13		
F8-DPB-CN[3]	Sol.	597	13	0.23	77
	Film	593	3		
F8-DPB-CN2[3]	Sol.	615	11	0.27	73
	Film	649	3		
BBEHBO-PPV[4]	Sol.	544	67	0.67	33
	Film	555	45		
MEH-PPV[4,5]	Sol.	572	49	0.35	65
	Film	595	17		
N-DPP-P[1]	Sol.	629	19	0.42	58
	Film	644	8		
N-DPP-T[1]	Sol.	686	18	0.31	69
	Film	703	6		
E-DPP-F[1]	Sol.	571	95	0.21	79
	Film	589	20		
E-DPP-P[1]	Sol.	572	74	0.31	69
	Film	641	23		
E-DPP-T[1]	Sol.	621	74	0.38	62
	Film	641	28		

Polymer Film CIE Coordinates

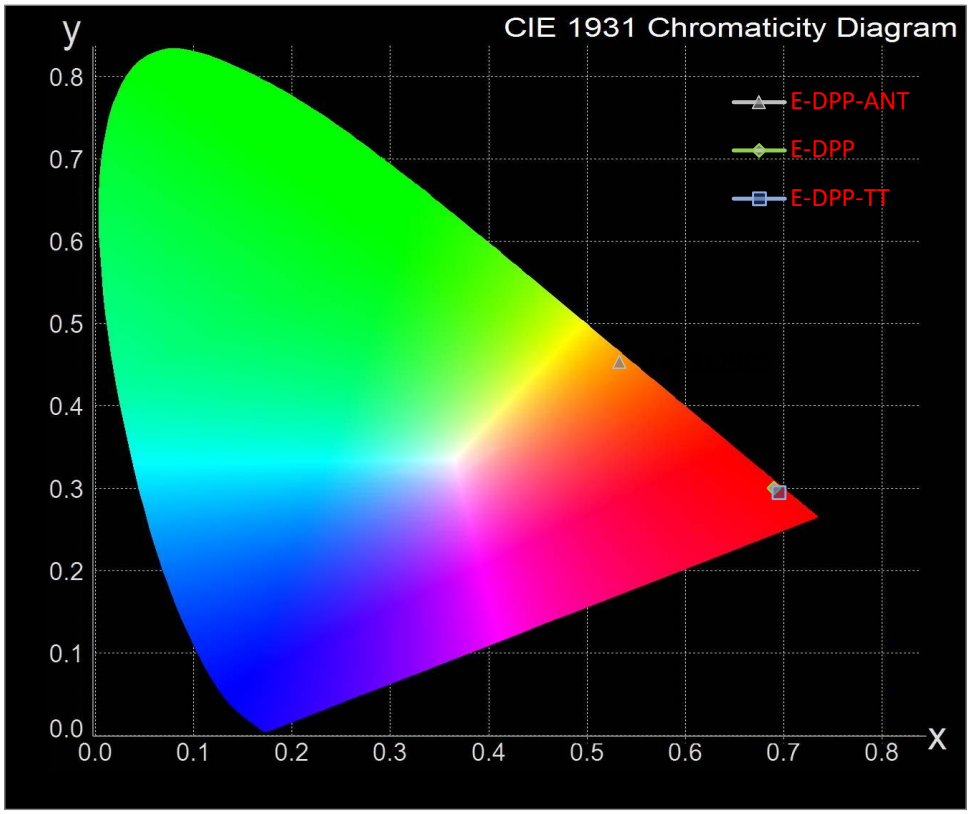

Figure S4. The CIE coordinates of E-DPP (green square), E-DPP-TT (blue square) and E-DPP-ANT (grey triangle).

Photophysical Data

E-DPP Polymer

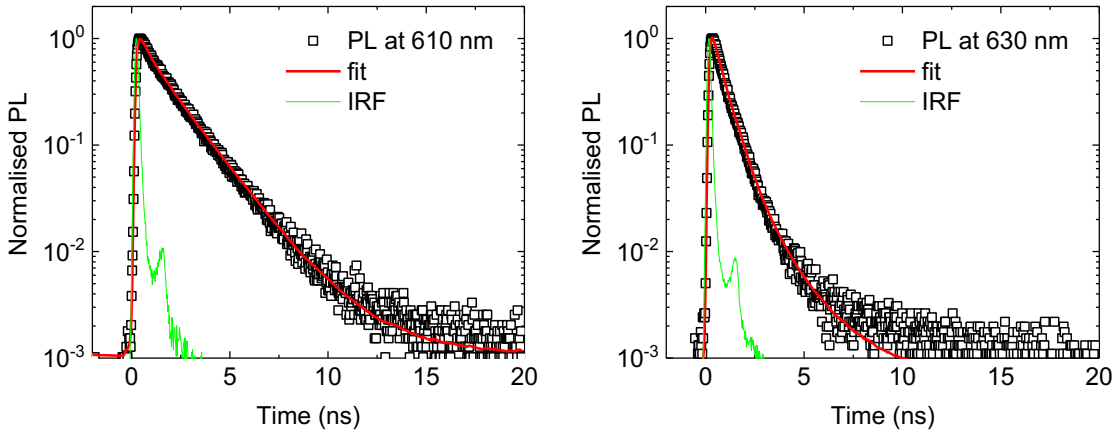

Figure S5. Semi-log plot of the transient PL (black squares) for E-DPP in solution (left) and thin film (right). The best fit (red curve) is achieved with a bi-exponential decay function with lifetime components $\tau1 = 0.54$ ns and $\tau2 = 1.76$ ns for the solution, with a tri-exponential decay function with lifetime components $\tau1 = 0.04$ ns, $\tau2 = 0.53$ ns and $\tau3 = 1.39$ ns for the thin film. The instrument response function is indicated in green. PL decays were collected via time-correlated single photon counting (TCSPC) with an Edinburgh Instruments Lifespec2, by exciting the samples with a 445-nm ps-pulsed laser diode.

E-DPP-TT Polymer

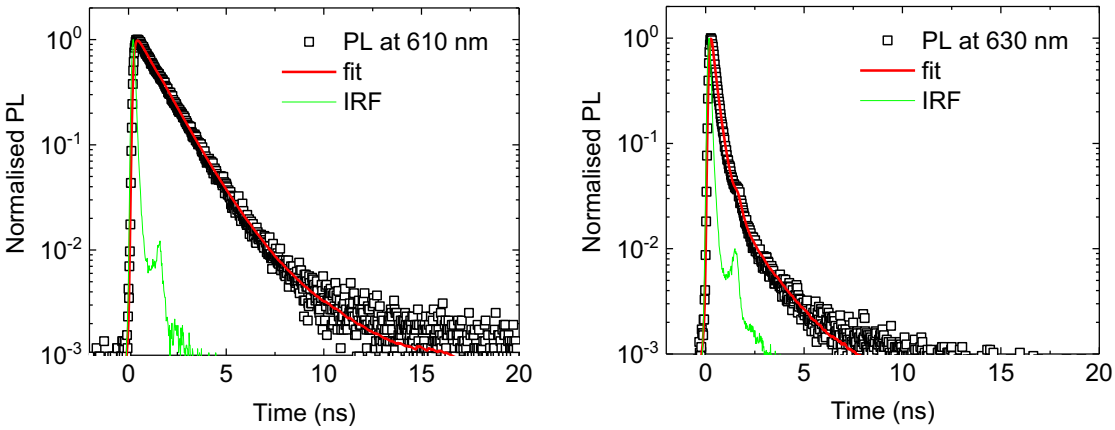

Figure S6. Semi-log plot of the transient PL (black squares) for E-DPP-TT in solution (left) and thin film (right). The best fit (red curve) is achieved with a bi-exponential decay function with lifetime components $\tau1 = 1.19$ ns and $\tau2 = 3.04$ ns for the solution. For the film, the transient PL data could be fit using a triexponential decay with lifetime components $\tau1 = 0.08$ ns, $\tau2 = 0.28$ ns and $\tau3 = 1.57$ ns. The instrument response function is indicated in green. The instrument response function is indicated in green. PL decays were collected via time-correlated single photon counting (TCSPC) with an Edinburgh Instruments Lifespec2, by exciting the samples with a 445-nm ps-pulsed laser diode.

E-DPP-ANT Polymer

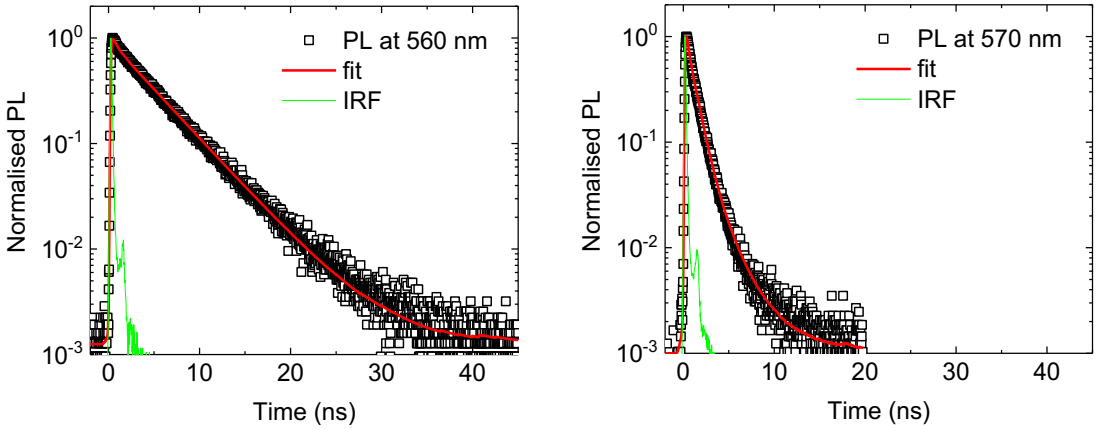

Figure S7. Semi-log plot of the transient PL (black squares) for E-DPP-ANT in solution (left) and thin film (right). The best fit (red curve) is achieved with a bi-exponential decay function with lifetime components $\tau1 = 0.56$ ns and $\tau2 = 4.60$ ns for the solution. For the film, the transient PL data could be fit using a triexponential decay with lifetime components $\tau1 = 0.18$ ns, $\tau2 = 0.83$ ns and $\tau3 = 2.11$ ns. The instrument response function is indicated in green. PL decays were collected via time-correlated single photon counting (TCSPC) with an Edinburgh Instruments Lifespec2, by exciting the samples with a 445-nm ps-pulsed laser diode.

Table S2. Fluorescence quantum yields of solutions of **E-DPP**, **E-DPP-TT** and **E-DPP-ANT** in different solvents. [a]Measured using an integrating sphere. [b]Measured relative to the chloroform solutions using a single point calculation. [c]The polymer does not dissolve in this solvent. **E-DPP** and **E-DPP-TT** were excited at 520 nm and **E-DPP-ANT** was excited at 500 nm.

Polymer	Solvent	Φ_F (%)
E-DPP	Chloroform	51±5[a]
	THF	49±5[b]
	Toluene	--[c]
E-DPP-TT	Chloroform	71±7[a]
	THF	58±6[b]
	Toluene	--[c]
E-DPP-ANT	Chloroform	57±6[a]
	THF	73±7[b]
	Toluene	66±6[b]

HOMO and LUMO Distributions

The following data was calculated using B3LYP/6-31G*.

E-DPP Polymer

LUMO (-2.18 eV)

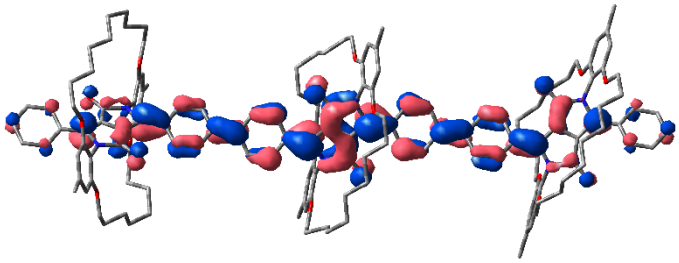

HOMO (-4.55 eV)

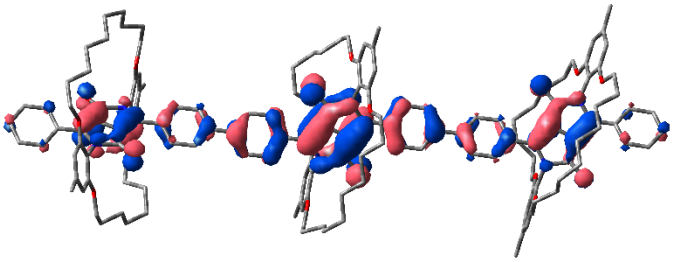

E-DPP-TT Polymer

LUMO (-2.35 eV)

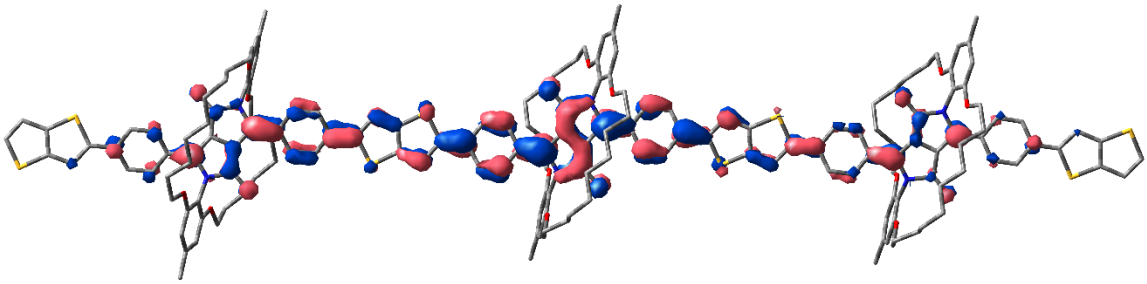

HOMO (-4.57 eV)

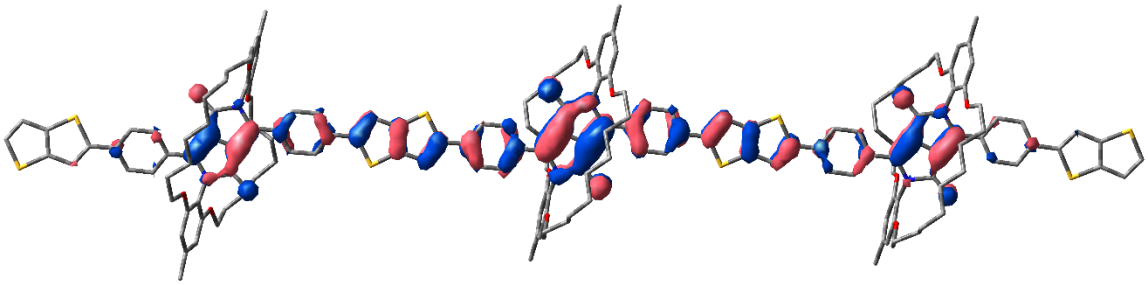

E-DPP-ANT Polymer

LUMO (-2.01 eV)

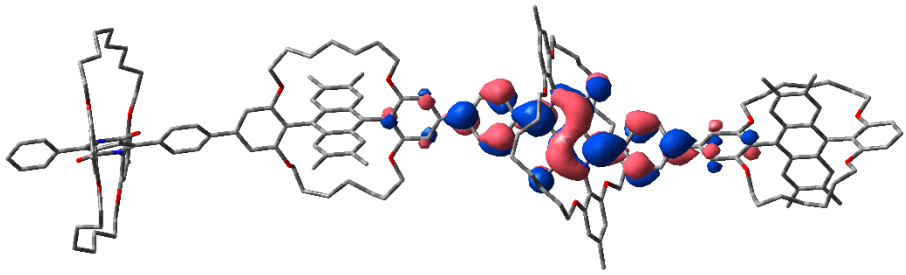

HOMO (-4.59 eV)

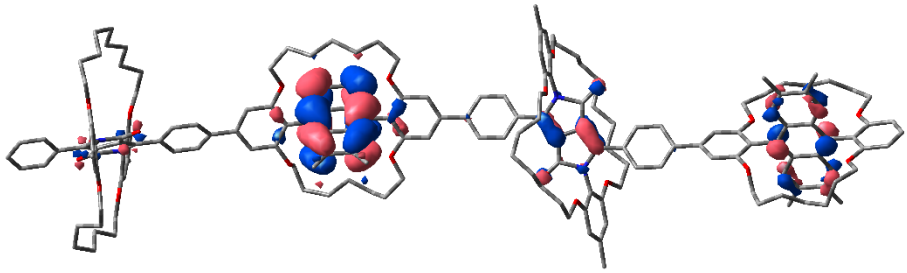

HOMO-2 (-4.66 eV)

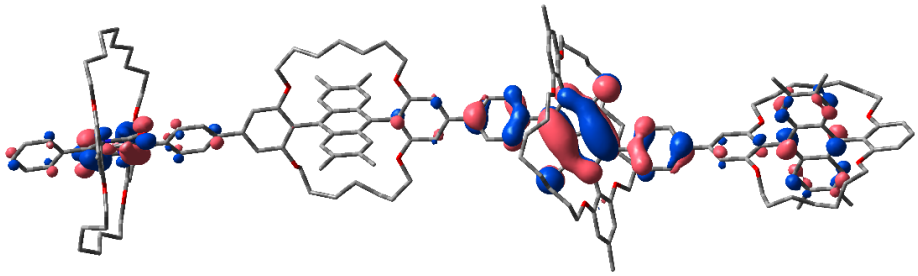

HOMO-3 (-4.67 eV)

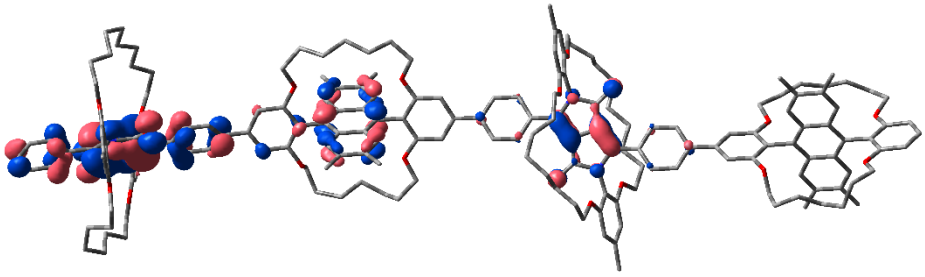

TD-DFT Data

The following data was calculated using B3LYP/6-31G*.

Table S3. TD-DFT data for E-DPP.

No.	Transition	Energy (cm^{-1})	Wavelength (nm)	Osc. Strength	Orbital contributions
1	$S_0 \rightarrow T_1$	9241	1082	0	HOMO → LUMO (60%), H-2 → L+2 (20%), H-1 → L+1 (14%), H-2 → LUMO (4%), HOMO → L+2 (3%).
2	$S_0 \rightarrow T_2$	9704	1030	0	H-2 → L+1 (22%), H-1 → LUMO (31%), H-1 → L+2 (20%), HOMO → L+1 (27%)
3	$S_0 \rightarrow T_3$	9937	1006	0	H-2 → LUMO (37%), H-1 → L+1 (33%), HOMO → L+2 (28%)
4	$S_0 \rightarrow S_1$	17049	587	1.7820	HOMO → LUMO (98%)

Table S4. TD-DFT data for E-DPP-TT.

No.	Transition	Energy (cm^{-1})	Wavelength (nm)	Osc. Strength	Orbital contributions
1	$S_0 \rightarrow T_1$	8837	1132	0	HOMO → LUMO (48%) H-2 → L+2 (24%), H-1 → L+1 (17%), H-2 → LUMO (2%) HOMO → L+2 (2%)
2	$S_0 \rightarrow T_2$	9048	1105	0	H-2 → L+1 (21%), H-1 → LUMO (26%), H-1 → L+2 (20%), HOMO → L+1 (25%)
3	$S_0 \rightarrow T_3$	9189	1088	0	H-2 → LUMO (34%), H-1 → L+1 (28%), HOMO → L+2 (30%)
4	$S_0 \rightarrow T_4$	15256	655	0	H-3 → LUMO (23%), HOMO → L+3 (17%) H-4 → L+1 (5%), H-4 → L+3 (3%), H-2 → L+1 (9%), H-1 → LUMO (7%), H-1 → L+2 (7%), H-1 → L+4 (3%), HOMO → L+1 (9%)
5	$S_0 \rightarrow S_1$	15714	632	3.9212	HOMO → LUMO (90%), H-1 → L+1 (7%)

Table S5. TD-DFT data for E-DPP-ANT.

No.	Transition	Energy (cm^{-1})	Wavelength (nm)	Osc. Strength	Orbital contributions
1	$S_0 \rightarrow T_1$	9957	1046	0	H-3 → LUMO (14%), H-2 → LUMO (68%), HOMO → LUMO (13%), H-1 → LUMO (4%)
2	$S_0 \rightarrow T_2$	9673	1033	0	H-3 → L+1 (73%), H-2 → L+1 (20%), HOMO → L+1 (5%)
3	$S_0 \rightarrow T_3$	14139	707	0	H-1 → L+3 (11%), HOMO → L+2 (20%), HOMO → L+3 (48%), H-3 → L+2 (3%), H-3 → L+3 (7%), H-1 → L+2 (4%)
4	$S_0 \rightarrow T_4$	14144	532	0	H-1 → L+2 (53%), H-1 → L+3 (22%), H-2 → L+2 (6%), H-2 → L+3 (2%), HOMO → L+2 (8%), HOMO → L+3 (4%)
5	$S_0 \rightarrow S_1$	18801	531	0.2406	HOMO → LUMO (95%)
6	$S_0 \rightarrow T_5$	18846	529	0	H-1 → LUMO (25%), HOMO → LUMO (66%), H-3 → LUMO (6%)
7	$S_0 \rightarrow T_6$	18900	529	0	H-2 → LUMO (10%), H-1 → LUMO (69%), HOMO → LUMO (18%)
8	$S_0 \rightarrow S_2$	18904	522	0.0131	H-1 → LUMO (97%)
9	$S_0 \rightarrow S_3$	19143	522	0.0666	H-1 → L+1 (16%), HOMO → L+1 (79%), H-3 → L+1 (3%)
10	$S_0 \rightarrow T_7$	19146	510	0	H-1 → L+1 (14%), HOMO → L+1 (75%), H-3 → L+1 (9%)
11	$S_0 \rightarrow S_4$	19626	492	1.1482	H-3 → LUMO (17%), H-2 → LUMO (78%)

GPC Chromatograms

E-DPP Polymer

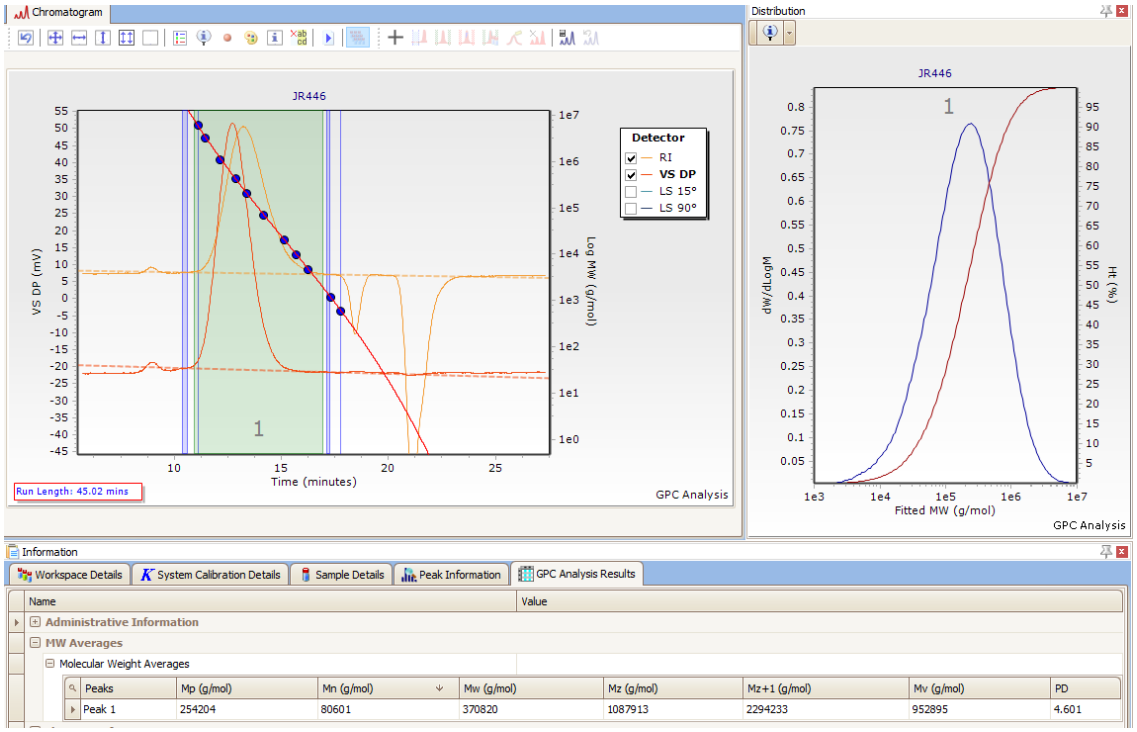

Peaks	Mp (g/mol)	Mn (g/mol)	Mw (g/mol)	Mz (g/mol)	Mz+1 (g/mol)	Mv (g/mol)	PD
Peak 1	254204	80601	370820	1087913	2294233	952895	4.601

E-DPP-TT Polymer

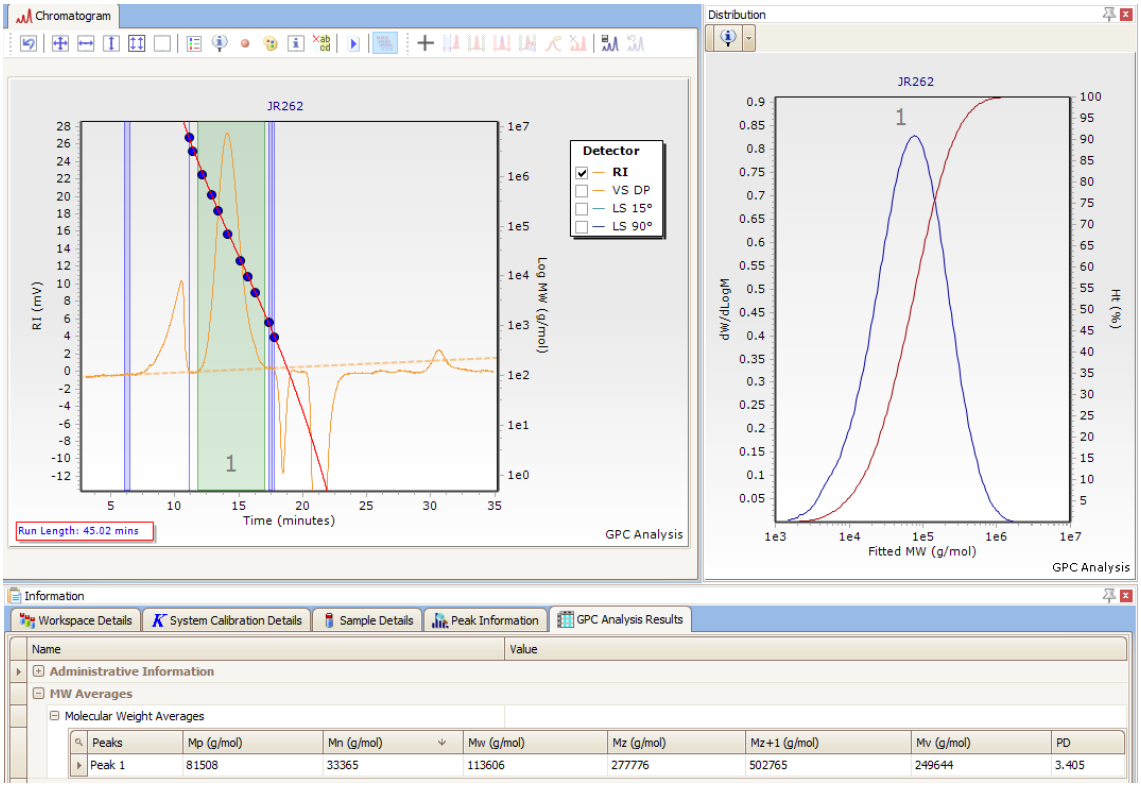

Peaks	Mp (g/mol)	Mn (g/mol)	Mw (g/mol)	Mz (g/mol)	Mz+1 (g/mol)	Mv (g/mol)	PD
Peak 1	81508	33365	113606	277776	502765	249644	3.405

E-DPP-ANT Polymer

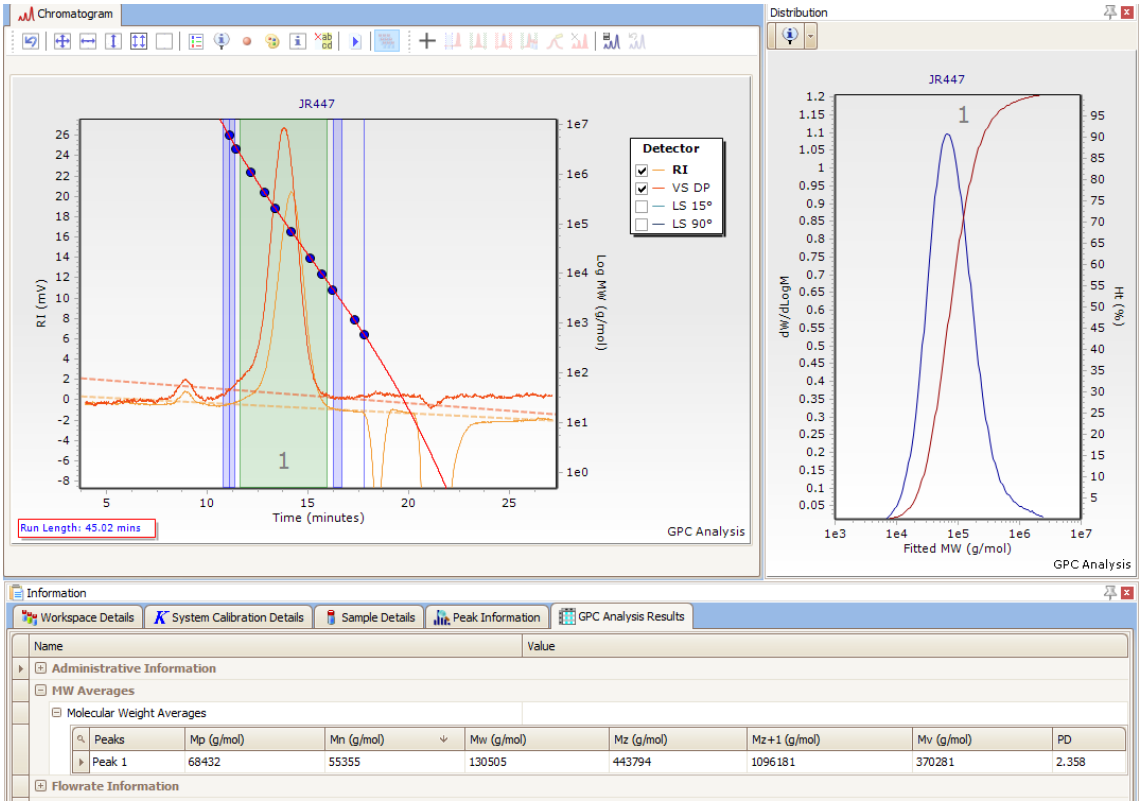

Peaks	Mp (g/mol)	Mn (g/mol)	Mw (g/mol)	Mz (g/mol)	Mz+1 (g/mol)	Mv (g/mol)	PD
Peak 1	68432	55355	130505	443794	1096181	370281	2.358

References

(1) Leventis, A.; Royakkers, J.; Rapidis, A. G.; Goodeal, N.; Corpinot, M. K.; Frost, J. M.; Bučar, D.-K. K.; Blunt, M. O.; Cacialli, F.; Bronstein, H. Highly Luminescent Encapsulated Narrow Bandgap Polymers Based on Diketopyrrolopyrrole. *J. Am. Chem. Soc.* **2018**, *140* (5), 1622–1626.

(2) Pan, C.; Sugiyasu, K.; Wakayama, Y.; Sato, A.; Takeuchi, M. Thermoplastic Fluorescent Conjugated Polymers: Benefits of Preventing π-π Stacking. *Angew. Chemie - Int. Ed.* **2013**, *52* (41), 10775–10779.

(3) Bera, M. K.; Chakraborty, C.; Malik, S. Solid State Emissive Organic Fluorophores with Remarkable Broad Color Tunability Based on Aryl-Substituted Buta-1, 3-Diene as the Central Core. *J. Mater. Chem. C* **2017**, *5* (27), 6872–6879.

(4) Vithanage, D. A.; Kanibolotsky, A. L.; Rajbhandari, S.; Manousiadis, P. P.; Sajjad, M. T.; Chun, H.; Faulkner, G. E.; O'Brien, D. C.; Skabara, P. J.; Samuel, I. D. W. Polymer Colour Converter with Very High Modulation Bandwidth for Visible Light Communications. *J. Mater. Chem. C* **2017**, *5* (35), 8916–8920.

(5) Ibnaouf, K. H. Excimer State of a Conjugated Polymer (MEH-PPV) in Thin Films. *Opt. Laser Technol.* **2013**, *48*, 401–404.